Polymer Chemistry

ROYAL SOCIETY OF CHEMISTRY

PAPER

View Article Online
View Journal | View Issue

Cite this: *Polym. Chem.*, 2025, **16**, 4013

Zwitterionic polymerization of glycolide catalyzed by pyridine

Hans R. Kricheldorf*[a] and Steffen. M. Weidner [b]

Received 30th July 2025,
Accepted 13th August 2025

DOI: 10.1039/d5py00762c

rsc.li/polymers

The usefulness of various N- and P-based catalysts for syntheses of cyclic polyglycolide *via* zwitterionic polymerization of glycolide was examined. Most catalysts produced discolored, largely insoluble polyglycolides consisting of cycles and unidentified byproducts. Soluble, cyclic polyglycolides were obtained using neat pyridine as catalyst at 120 °C, 100 °C, 80 °C, and even at 60 °C. The number-average molecular weights were extremely low and depended slightly on the glycolide-to-pyridine ratio. Three different mass distributions of the cycles were detected by mass spectrometry, depending on the reaction conditions. The cyclic polyglycolides were also characterized by differential scanning calorimetry (DSC) and small-angle X-ray scattering (SAXS) measurements. The SAXS data in combination with the mass spectra indicate that the majority of the cycles form extended-ring crystallites.

Introduction

The properties of cyclic polymers differ from those of their linear counterparts in various aspects.[1–11] Thus, research activities concerning the synthesis and characterization of cyclic polymers have increased considerably over the past fifty years. Two distinct synthetic strategies have been developed: ring-expansion polymerization, which is beyond the scope of this study, and cyclization *via* difunctional linear chains. The latter strategy can be divided into two versions. In version I, the linear intermediates are stable species that can be isolated, and cyclization occurs in a separate second step. This approach is characterized by the formation of "guest–host" copolymers, wherein the guest monomer is derived from fragments of the functional end groups.[6,7] However, as demonstrated for poly(L-lactide), the physical properties of such guest copolymers may differ greatly from those of true homopolymers.[12]

Version II is characterized by ring-opening polymerization (ROP), which yields reactive linear intermediates that undergo polycondensation and cyclization simultaneously. This version is called the ROPPOC (Ring-Opening Polymerization with Polycondensation and Cyclization) method. As defined and illustrated in a previous review,[13] the ROPPOC method may involve ionic or covalent end groups. The variant with two ionic end groups is called zwitterionic polymerization (ZP). The first formulation of a zwitterionic polymerization mechanism was the polycondensation mechanism proposed by Elias and Bühler in 1970 (see Scheme 1), which was not supported by any experimental evidence.[14,15] Four years later, Kricheldorf reported the first formulation and realization of a zwitterionic ring-opening polymerization (ROP) based on the pyridine-catalyzed ROP of proline *N*-carboxyanhydrosulfide (NTA, Scheme 2).[16]

Further pyridine-catalyzed ROPs of *N*-carboxyanhydrides (NCAs) and *N*-thiocarboxyanhydrides (NTAs) of various amino acids were also performed,[17] but the cyclic architecture of the resulting polypeptides was not evident at that time. However, a re-investigation of previous experiments, as well as new experiments involving various amino acid NCAs, proved the cyclic topology by means of MALDI-TOF mass spectrometry in 2005 and 2006.[18–20] Earlier, the first author had studied pyridine- and trialkylamine-catalyzed polymerizations of S-carboxyanhydrides of mercaptoacetic acid and mercapto-D,L-lactic acid.[21,22] Although a zwitterionic mechanism was not formulated, a detailed reinves-

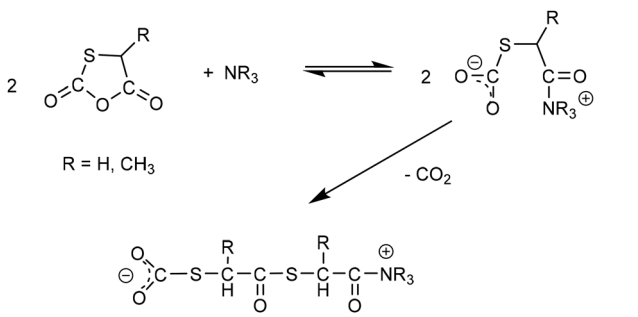

Scheme 1 Zwitterionic polycondensation mechanism formulated in ref. 15 for the trialkylamine-catalyzed polymerization of thioglycolic acid *S*-carboxyanhydride (1,3-oxathiolane-2,5-dione).

[a]*University of Hamburg, Institute for Technical and Macromolecular Chemistry, Bundesstrasse 45, D-20146 Hamburg, Germany. E-mail: hrkricheldorf@aol.de*
[b]*Federal Institute for Materials Research and Testing–BAM, Richard Willstätter Strasse 11, D-12489 Berlin, Germany*

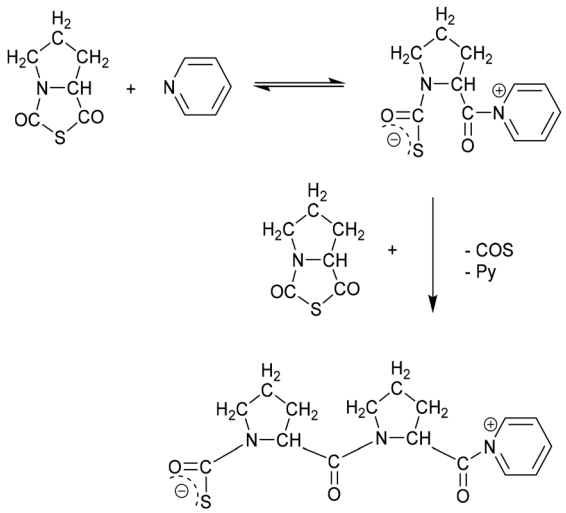

Scheme 2 Mechanism of a pyridine-catalyzed zwitterionic polymerization of proline *N*-carboxy anhydrosulfide formulated in ref. 16.

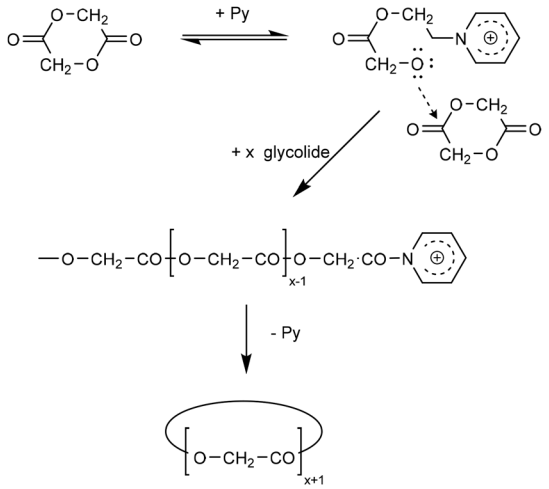

Scheme 3 Mechanism of pyridine-catalyzed ring-opening polymerization (ROP) of glycolide.

tigation in 2007 proved that poly(thioglycolide) and poly(thio-D,L-lactide), prepared in this manner, indeed had a cyclic topology due to a zwitterionic polymerization mechanism.[23] Further cyclic polyesters were prepared by pyridine-catalyzed ROPs of hydroxy acid *O*-carboxyanhydrides.[24–26] Cyclic anhydrides and anhydrosulfides are strong electrophiles that are sensitive to traces of pyridine and substituted pyridines. However, pyridines are not reactive enough to catalyze zwitterionic polymerizations of cyclic esters, which are far less electrophilic, such as δ-valerolactone, ε-caprolactone, and cyclic carbonates. N-heterocyclic carbenes and amidines are effective zwitterionic catalysts for these monomers, as demonstrated by Waymouth *et al.*[27–33] However, the high basicity of these catalysts causes racemization of L-lactide at room temperature. Thus, these catalysts are ineffective for preparing optically pure cyclic poly(L-lactide). This disadvantage is, of course, not relevant for other cyclic esters. Zwitterionic polymerizations of lactide by modified carbenes and other catalysts have also been reported by other research groups.[34–38]

Glycolide is the most reactive cyclic ester commercially available. Beginning with the work of Gilding and Reed,[39] it was found that its incorporation rate is far higher than that of lactide when the two monomers are co-polymerized. Furthermore, racemization is not a problem. Thus, the authors investigated whether zwitterionic polymerizations of glycolide could be catalyzed by nucleophilic tertiary amines or phosphines at temperatures above 100 °C in bulk (Scheme 3).

Experimental

Materials

Glycolide was purchased from Polyscience (Hirschberg, Germany) and recrystallized from a mixture of anhydrous THF and toluene (1/2 v/v). Anhydrous THF, toluene and pyridine were purchased from Thermo-Scientific Fisher (Schwerte Germany). *N*-Dimethylpyridine (DMAP), 1,2-dimethyl imidazole (DMI), triphenylphosphine (TPP) were purchased from Sigma-Aldrich and used as received.

Polymerization with DMAP

DMAP (0.1 mmol) and GL (40 mmol) were weighed into a flame-dried 50 mL round-bottom flask under a blanket of argon, and a magnetic bar was added. The reaction vessel was immersed into an oil bath thermostated at 120 °C. Following a 24 hour period, the discolored solid PGA was extracted with a spatula or pincer and characterized in its pristine state. Analogous polymerizations were conducted at 150 and 180 °C for a duration of 2 hours.

The polymerizations catalyzed by DMIM (0.1 mmol) or TPP (0.1 mmol) were conducted analogously.

Polymerizations with pyridine

GL (40 mmol) was weighed into a flame-dried 50 mL Erlenmeyer flask under a blanket of argon. Then, a magnetic bar was added, and pyridine (4, 40, 160, or 400 mmol) was injected. The reaction vessel was immersed into an oil bath thermostated at 120 °C. The PGA prepared with A GL/Py ratio of 10/1 or 1/1 was isolated as a crystalline plaque. This plaque was subsequently crushed in a mortar. The PGAs from the other experiments were isolated as crystalline powders. Following a 30 minute reflux process in chlorobenzene, the PGAs were isolated as brownish or off-white materials and subsequently dried at 80 °C *in vacuo*.

Measurements

The MALDI TOF mass spectra were measured with Autoflex maX mass spectrometer (Bruker Daltonik GmbH, Bremen, Germany) equipped with a Smartbeam laser (λ = 355 nm). All spectra were recorded in the positive ion linear mode. The MALDI stainless steel targets were prepared from solutions of PGA in HFIP and doped with potassium trifluoroacetate (2 mg

mL^{-1}). Typically, 20 μL of sample the solution, 2 μL of the potassium salt solution and 50 μL of a solution of *trans*-2-[3-(4-*tert*-butylphenyl)-2-methyl-2-propenylidene] malononitrile (DCTB, 20 mg mL^{-1} in HFIP) serving as matrix were mixed in an Eppendorf vial. 1 μL of the corresponding solution was deposited on the MALDI target. FlexControl (Bruker Daltonik GmbH) was used to record spectra by accumulating 2000 single laser shots recorded at 4 different positions.

The GPC measurements were performed in a modular system kept at 30 °C consisting of an isocratic pump (Agilent, USA) running with a flow rate of 0.5 mL min^{-1} and a refractive index detector (RI-501-Shodex). HFIP was used as eluent. Samples were manually injected (100 μL, *ca.* 2–4 mg mL^{-1}). For instrument control and data calculation WinGPC software (Polymer Standard Service-PSS now Agilent, Mainz, Germany) was used. The calibration was performed using a polymethylmethacrylate (PMMA) standard set (Polymer Standards Service – PSS, Mainz).

The DSC heating traces were recorded on a (with indium and zinc freshly calibrated) Mettler-Toledo DSC-1 equipped with Stare Software-11 using a heating rate of 10 K min^{-1}. Only the first heating traces were evaluated.

The SAXS measurements were performed using our in-house SAXS/WAXS apparatus equipped with an Incoatec™ X ray source IμS and Quazar Montel optics. The wavelength of the X ray beam was 0.154 nm and the focal spot size at the sample position was 0.6 mm^2. The samples were measured in transmission geometry and were recorded with a Rayonix™ SX165 CCD-Detector. The SAXS measurements were performed at sample-detector distance of 1.6 m and the accumulation was 1200 s for each position. DPDAK, a customizable software for reduction and analysis of X-ray scattering data sets was used for gathering 1D scattering curves.[40] For the evaluation of the crystallinity of the samples the data were imported in Origin™ and analyzed with the curve fitting module. The SAXS curves were converted into Kratky plots. The long periods of the lamellar domains were determined by the q values of the reflection maxima.

Results and discussion

Screening of catalysts

A preliminary screening was conducted using four potential catalysts with different structures: 4-dimethylaminopyridine, 1,2-dimethylimidazole, triphenylphosphine, and tris(4-nonylphenyl)phosphite. Expecting that glycolide would be difficult to polymerize using these potential catalysts, the first experiment with DMAP was conducted at 180 °C (no. 1, Table 1). Polymerization became observable after 5 minutes, with complete solidification of the reaction mixture within 15 minutes. A dark brown product was formed that was not fully soluble in HFiP. However, the MALDI TOF mass spectra indicated that this product was predominantly composed of cyclic PGA (cPGA), at least within the low molar mass range. In the subsequent experiment, the temperature was reduced to 150 °C.

Table 1 ROPs of GL catalyzed with various aprotic nucleophiles

Exp. no.	Catalyst	GL/Cat	T (°C)	t (h)	T_m (°C).	ΔH_m (J g^{-1})
1	DMAP	200/1	180	0.5	221.3	103
2	DMAP	200//1	150	0.5	222.6	109
3	DMAP	200/1	120	24	191.6	36
5	1,2-DMI	200/1	120	24	—	—
6	TPP	200/1	150	3	—	—
7	TPP	200/1	120	3	—	—
8	TPP	100/1	120	3	—	—

This resulted in the formation of a product that exhibited an orange hue. However, even this PGA lacked complete solubility.

The mass spectrum exclusively exhibited peaks of cPGAs in the low molar mass range (Fig. 1). Especially remarkable is the mass distribution of the cycles, because even-numbered cycles are largely predominant over the full mass range. Such a mass spectrum was not observed in previous studies.[41–44] This finding suggests that the propagation rate may have exceeded that of the transesterification reaction, a notable observation given the elevated temperature and the results obtained with pyridine (see below).

Complete conversion at 180 or 150 °C entailed one melting endotherm in the DSC heating trace with a minimum around 222 °C (Fig. 2A). This value was also found for other cyclic PGAs. At 120 °C, the conversion with DMAP was incomplete, even after 24 hours, as demonstrated by a broad melting endotherm of unreacted glycolide, ranging from 50 to 90 °C, in the DSC heating trace (Fig. 2B), as well as a strong melting endotherm of polyglycolide (Fig. 2B).

An experiment with 1,2-DMI at 120 °C (no. 3, Table 1) produced a sample with nearly complete conversion after 24 hours. The mass spectrum displayed a predominance of cyclic PGAs below 3000 *m*/*z*; however, mass peaks of un-

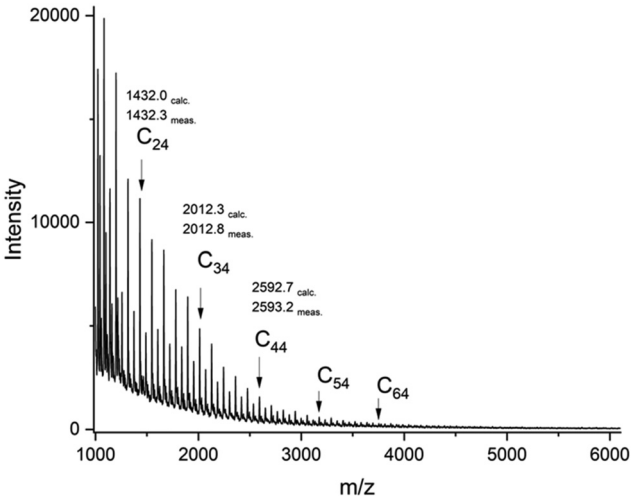

Fig. 1 MALDI TOF mass spectrum of cPGA prepared with DMAP in bulk at 150 °C (no. 2, Table 1).

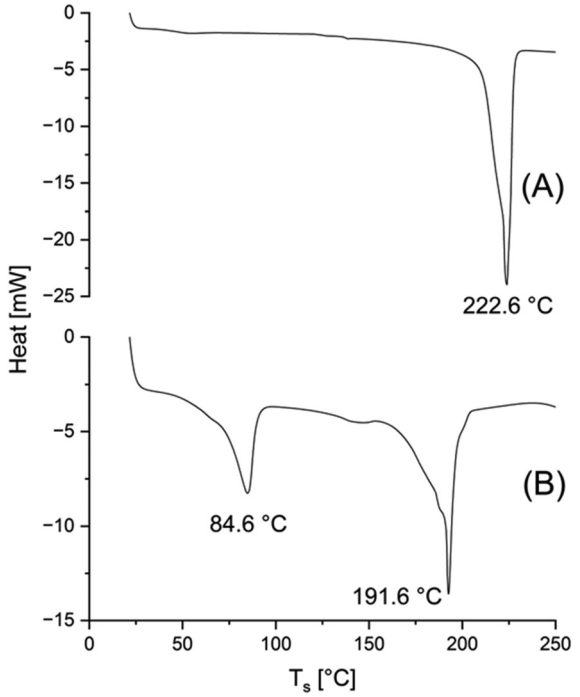

Fig. 2 DSC heating traces (1st heating) of (A) cPGA prepared with DMAP at 150 °C (no. 2, Table 1), (B) prepared with TPP at 150 °C (no. 6, Table 1).

identified linear species dominated at higher masses, and the reaction product exhibited an almost black discoloration. Finally, three experiments with TPP as the catalyst were conducted. All three experiments had the following features in common: the mass peaks of cyclic PGAs dominated the mass range up to *m*/*z* 5000 but were accompanied by mass peaks of at least three types of linear species. Furthermore, despite the relatively rapid solidification of the reaction mixture, conversions were apparently all below 50%, as indicated by a melting endotherm of glycolide in the DSC heating traces, even at 150 °C (in analogy to Fig. 2B). TNPP experiments were conducted at 120 °C, 150 °C, and 180 °C; however, all three experiments failed to yield PGA. In summary, this first series of experiments revealed that GL can be polymerized *via* a zwitterionic mechanism even at temperatures as low as 120 °C, but tertiary amines are needed as catalysts. However, due to the intense side reactions and strong discoloration, DMAP and 1,2-DMI were not promising catalysts for preparative purposes.

Polymerizations catalyzed with pyridine

Although we did not expect pyridine to be nucleophilic enough to catalyze a zwitterionic polymerization of GL at moderate temperatures, we conducted an experiment at 120 °C with an excess of pyridine. However, the boiling point of pyridine does permit a higher polymerization temperature in normal glassware. Surprisingly, after 24 hours, this experiment (no. 3, Table 2) yielded a brown PGA dispersed as a crystalline powder in the excess pyridine. This PGA was completely soluble in HFiP, and the mass spectrum revealed peaks exclusively of cycles up to *m*/*z* 4000 (Fig. 4A). These positive results stimulated further experiments involving variations in the GL/Py ratio and temperature (Table 2). Polymerizations with GL/Py ratios of 1/1 or 10/1 produced solids within approximately 0.5 hours, and the resulting PGAs were isolated after two hours. Polymerizations conducted with lower GL concentrations were worked up after 22 hours, and the resulting PGAs were isolated as crystalline powders.

Table 2 Pyridine-catalyzed polymerizations of GL

Exp. no.	GL/Py	*T* (°C)	*t* (h)	Yield (%)	M_n	M_w
1	1//4	120	2	92	1350	2100
2	1/1	120	2	95	1400	2250
3A	10/1	120	2	91	1320	2300
3B	10/1	120	24	94	1350	2400
4A	20/1	120	2	92	1400	2450
4B	20/1	120	24	94	1450	2700
5A	40/1	120	2	93	1600	3100
5B	40/1	120	24	95	1750	3750
6	100/1	120	24	93	1850	3600
7	200/1	120	24	96	1800	3600
8	400/1	120	24	Low conv.	—	—
9	1/1	100	24	92	1450	2200
10	1/1	80	24	65	1400	2200
11[a]	1/1	80	24	29	1450	2700
12	1/2	60	24	11	—	—

[a] Chlorobenzene was added in a 1/1 (v/v) ratio relative to pyridine.

Three more experiments were conducted at lower temperatures with a GL/Py ratio of 1 : 1 (no. 9–11, Table 2). At 100 °C, the initially clear solution turned cloudy after approximately one hour, and PGA began to crystallize on the glass walls of the reaction vessel. The same phenomenon was observed at 80 °C after two hours. After 22 hours, the resulting PGAs were isolated as crystalline powders. Most PGAs prepared with pyridine were soluble in HFiP, and GPC measurements yielded extremely low molecular weights in all cases.

Two noteworthy trends emerged. First, the molecular weights increased slightly with increasing monomer concentration. Second, most elution curves were bimodal, as illustrated in Fig. 3, or in a few cases even trimodal (Fig. S1 and S2, SI). Surprisingly, the dispersities were rather low, mainly ranging from 1.25 to 1.40, despite the bimodality of the GPC curves. The low molecular weights have two advantages. First, the MALDI TOF mass spectra are representative of most of the components in the PG samples. Second, the low molecular weights indicate that pyridine-catalyzed polymerization is a complementary approach to polymerizations catalyzed with tin compounds, which yield extremely high molecular weight PGAs.[41,42] Such low molecular weights are, of course, useless for any mechanical application, but may be of interest for 3D printing of biodegradable medical devices by photopolymerization[45] or in academic studies such as crystallization kinetics.

The mass spectra of all samples exclusively displayed peaks of cycles and most spectra were quite similar to that of Fig. 4A However, the PGAs prepared at 100 °C or below displayed a

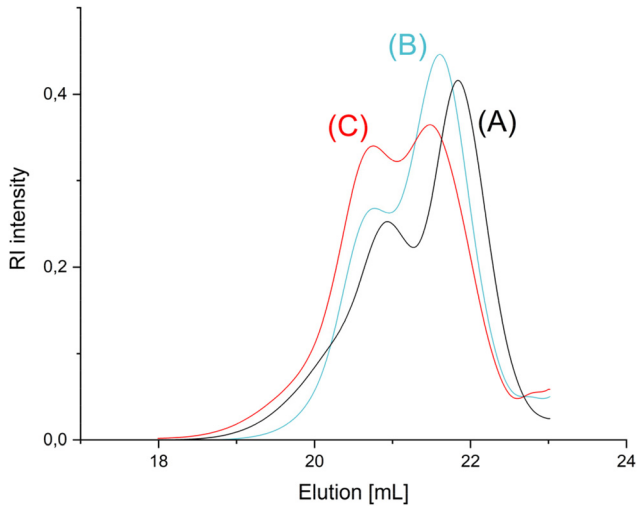

Fig. 3 GPC elution curves of (A) no. 11, Table 2, (B) no. 10, Table 2, (C) no. 12, Table 2.

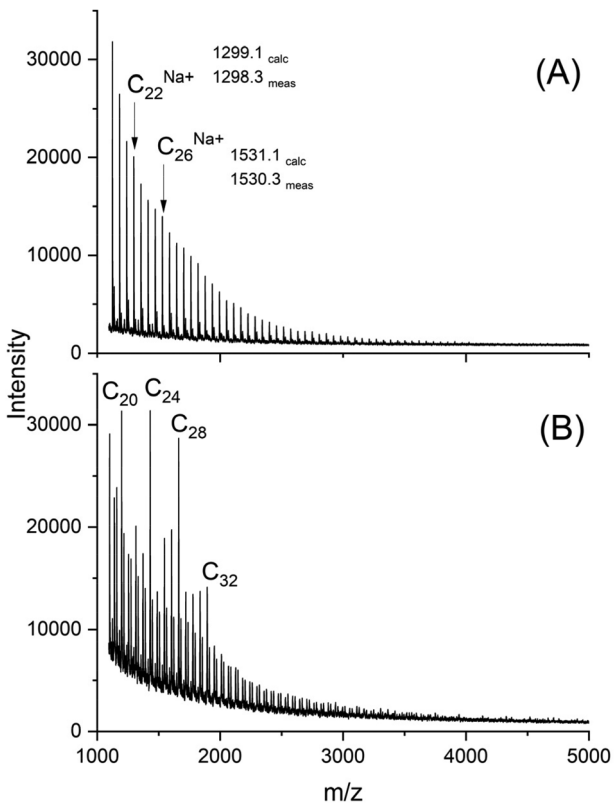

Fig. 4 MALDI-TOF mass spectra of cPGAs prepared with pyridine at 120 °C (A) no. 3, Table 2, (B) after annealing with $SnOct_2$ at 140 °C for 1 h (no. 1A, Table 4).

predominance of the even-numbered cycles over the odd-numbered ones quite analogous to the spectrum of Fig. 1 (and Fig. S3, S4). Unfortunately, the signal-to-noise (S/N) ratios of these mass spectra were poor compared to those of polylactide. The poor performance of PGA in MALDI TOF mass spectrometry results from the strong interchain forces between the densely packed PGA chains, a phenomenon that has also been observed in previous studies based on other catalysts.[41–44]

Since all cyclic PGA samples prepared with pyridine exhibited a reddish or brownish discoloration that appeared to be inherent to the liquid phase, two attempts were made to remove the discoloration. The first attempt involved extracting the color using refluxing anhydrous dichloromethane or toluene. However, this method was not very successful because it was difficult to obtain the PGAs from experiments No. 1 and 2 (Table 2) as fine powders. Another attempt to purify the PGAs involved dissolution in HFiP, followed by precipitation in a 50/50 (v/v) mixture of THF and toluene. This method yielded PGA in the form of an ochre or grayish powder. The color and intensity of the discoloration decreased with the temperature. The PGA isolated from the 80 °C experiment had an ochre color and the PGA obtained at 60 °C showed a yellowish discoloration. The discoloration is most likely due to side reactions initiated by deprotonation (Scheme 3). This hypothesis is supported by the following observations. Deep red discoloration was also observed when L-lactide was heated in refluxing pyridine. After 24 hours, no polymerization was detectable, but the lactide was largely racemized, as indicated by a broad melting endotherm between 25 and 35 °C (after complete evaporation of the pyridine *in vacuo*), which is typical of contaminated *meso*-lactide (L-lactide has a T_m of 98–99 °C, and rac-D,L-lactide has a T_m of 125–126 °C). Furthermore, a reddish/brownish discoloration appears rapidly when a trialkyl amine is added to an aliphatic acid chloride solution with a proton in the α-position. Since H. Staudinger's work, it has been known that this reaction yields ketenes by dehydrohalogenation. The ketenes, which can also be formed from glycolide (see Scheme 4), cause a variety of side reactions. Considering the risk of deprotonation and subsequent side reactions, the low basicity of pyridine is advantageous compared to the more basic amines used in this study.

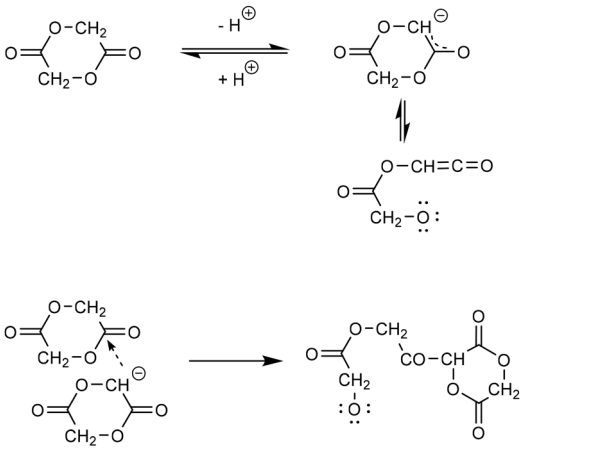

Scheme 4 Reversible deprotonation of glycolide and subsequent side reaction.

Annealing experiments

The molecular weight distribution (MWD) of all cyclic poly(glycolic acid) (PGA) polymers prepared using pyridine or dimethylaminopropylamine (DMAP) resembles the Schulz–Flory distribution, with a maximum in the oligomer range and a steady exponential decay with increasing degree of polymerization (Fig. 1 and 3A). However, cyclic PGAs prepared with tin catalysts in bulk at higher temperatures displayed an "saw-tooth pattern" (STP) of mass peaks in the *m*/*z* 1000–2500 range (Fig. 4B).[41–44] In analogy to the STP of cyclic polylactides, this pattern is explained by the formation of extended-ring crystallites consisting of cycles with a similar ring size because such crystallites are thermodynamically favored due to their smooth surface and lack of internal defects (Fig. 5A). For PLA, it was found, and for PGA it was assumed, that these extended-ring crystallites displaying a STP were formed by transesterification reactions on the surface of the crystallites. To test this hypothesis, cPGA prepared in pyridine (no. 3, Table 2) was dissolved in HFiP, and $SnOct_2$ was added at a GL/Sn ratio of 250 : 1.

The HFiP was evaporated, and the crystallized residue was annealed at 140 °C for one or six hours (Table 4). Regardless of the time, the mass spectra of both samples displayed the STP known from cPGAs prepared at high temperatures in bulk (Fig. 4B).[41–44] Characteristic for the STP of annealed cPGAs is the preferential formation of cycles with DP values of 20, 24, 28, 32, and 36 GA units. The reason, why these ring sizes represent a thermodynamic optimum remains unclear at this time. However, these experiments confirm the authors' previous hypothesis.

In addition to the STP, the mass spectrum obtained after annealing with $SnOct_2$ displayed another interesting phenomenon. Linear byproducts were formed, and these linear PGAs exhibited a mass distribution that corresponded to the most probable distribution initially calculated by Flory.[46] The finding that STP cycles and linear chains had two different mass distributions indicates that they form separate crystallites. This phenomenon was quite recently also observed for alcohol-initiated and $SnOct_2$-catalyzed ROPs of GL[43] and it was found for the simultaneous formation of cyclic and linear PLAs.[47,48]

Finally, it should be noted that considering Fig. 1 and 4, the mass spectra presented in this work display three different distribution patterns. In previous publications only the pattern of Fig. 4B was observed.[41–44]

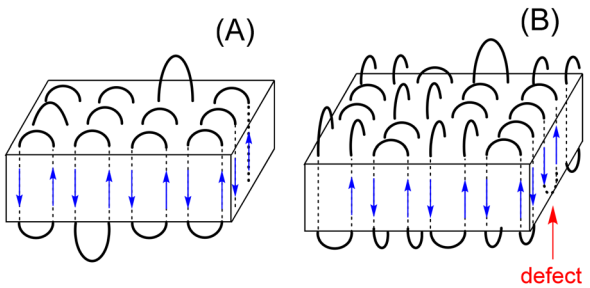

Fig. 5 Schematic illustration of (A): an extended-ring crystallite made up by cycles of nearly identical ring size, (B) a crystallite formed by once-folded cycles.

X-ray measurements

Since the authors prepared cyclic PGAs for the first time and synthesized them at various temperatures, it made sense to compare the WAXS powder patterns. The cPGAs prepared in this study showed bimodal DSC traces (see Fig. 6) and GPC elution curves (see Fig. 3). In contrast, cPGAs prepared with tin catalysts in bulk at higher temperatures had monomodal DSC traces and monomodal GPC elution curves. The WAXS patterns of samples no. 3, 5, and 8, however, were identical, as were those of a high molar mass cPGA prepared *via* ring-expansion polymerization at

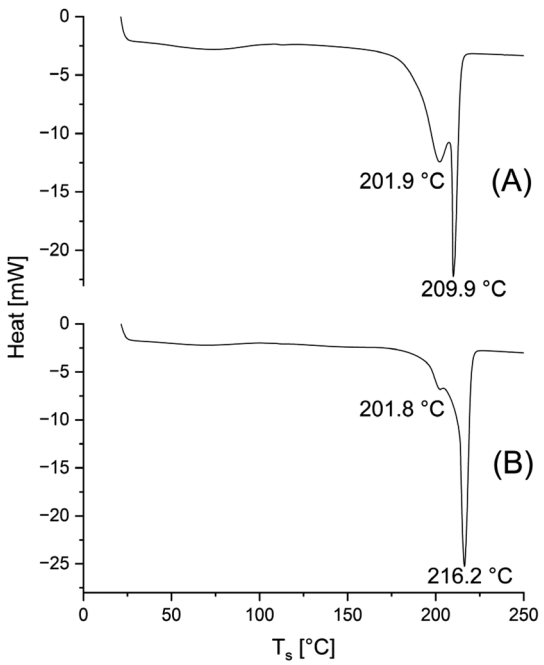

Fig. 6 DSC heating traces (1st heating) of cPGA prepared with pyridine at 120 °C: (A) GL/Py = 1/4, (no. 2, Table 2), (B) GL/Py = 1/10 (no. 1, Table 2).

Table 3 DSC and SAXS measurements of pyridine-catalyzed polymerizations of GL

Exp. No.	GL/Py	T (°C)	T_m (°C).	ΔH_m (J g^{-1})	Cryst. [a] (%)	L (nm)	l_c [b] (nm)
1	1/1	120	219.5	105	51	6.9	3.4
2	1//4	120	210.1	119	58	7.3	3.6
4	1/1	100	120.0	104	50	7.5	3.7
5	1/1	80	220.2	107	52	6.8	3.4
6	1/2	60	215.4	148	71	6.3	3.1
7	10/1	120	217.3	118.6	57	7.3	3.6
8	20/1	120	219.0	110.6	53	—	—
9	100/1	120	221.5	97.8	45	—	—
10	200/1	120	216.7	65.3	32	—	—

[a] Calculated with a ΔH_m^0 of 206 J g^{-1}. [b] Calculated from L by multiplication with the crystallinity.

Table 4 Annealing of cPGAs with addition of $SnOct_2$ (Gl/Cat = 250/1)

Exp. no.	Cat.	T (°C)	t (h)	T_m (°C)	ΔH_m (J g^{-1})	Cryst. [a] (%)	L (nm)	l_c [b] (nm)
1A	$SnOct_2$	140	1	216.5	122.7	60	6.3	3.1
1B	$SnOct_2$	140	6	215.7	135.5	65	6.1	3.0

[a] Calculated with a ΔH_m^0 of 206 J g^{-1}. [b] Calculated from L by multiplication with the crystallinity.

160 °C.[41,42] These results indicate that all cyclic PGAs adopt the crystal lattice of linear PGAs, which has antiparallel chain alignment and a planar zigzag chain conformation. The SAXS measurements yielded the *L*-values listed in Tables 3 and 4.

Regardless of topology or synthetic method, it is characteristic for PGA that the *L*-values are below 8 nm and the thickness of the crystallites (l_c) is low (typically <4 nm), much lower than in the case of PLA.[47,48] The long-distance values (L) measured for the cPGAs prepared with pyridine agree with this trend, as demonstrated by the *L*- and l_c-values listed in Tables 3 and 4. These samples are characterized by relatively broad and weak reflections, which suggest small crystallites and a low degree of crystallinity (in agreement with the DSC measurements), as illustrated by curve A in Fig. 7. Upon annealing at 140 °C, the first- and second-order reflections sharpened, indicating an improvement in the third-order within the spherulites (Fig. 7(B)).

The l_c values found for the cPGAs fit in with a sequence of 10–13 glycolyl units, sine the length of 10 repeat units amounts to 3.0 nm.[49] These degrees of polymerization (DPs) correspond, in turn, to ring sizes of 20–26 repeat units Since l_c values listed in Tables 3 and 4 only represent a rough estimation and since the thickness of the crystallites may cover a broad distribution, it is plausible that also slightly larger cycles having DPs up to 30 or32 may form extended-ring crystallites, whereas larger cycles have to fold at least once to fit in with a crystal thickness around 31–37 nm.

However, folding considerably reduces the perfection of the crystallites in two ways as illustrated in Fig. 5B. First, insufficient length of a folded ring may cause defects inside crystal lattice. Second, the surface has a lower degree of order, because the loops resulting from folding adopt an orientation perpendicular to the loops formally representing ring end groups. As mentioned above, the perfection of extended-ring crystallites has the consequence that they crystalize separately from linear chains. This phenomenon raises now the question, if extended-ring crystals also strictly exclude folded rings, so that cycles folding one or twice upon crystallization form separate crystallites. A detailed study of this problem was beyond the scope of this work and it will be difficult any way to find an analytical method allowing for solution of this problem. Nonetheless, this discussion illustrates, why low molar mass cyclic PGAs and PLAs are interesting substrates for studies of crystallization phenomena.

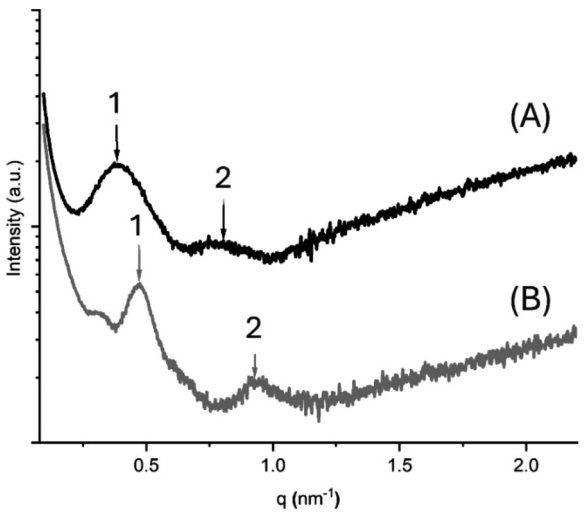

Fig. 7 SAXS curves of (A) cPGA No.1 Tables 2 and 3, (B) no. 1, Table 4.

Conclusions

These results demonstrate, for the first time, that the zwitterionic polymerization of cyclic esters can be catalyzed by the weakly nucleophilic compound pyridine. Cyclic polyglycolides can be produced through pyridine-catalyzed zwitterionic polymerization at temperatures of 120 °C or below. This synthetic method has the advantages of a simple procedure and an inexpensive, commercially available catalyst. The low molecular weights complement the high molecular weights achieved with tin catalysts, as previously reported.[41,42] Such low molecular weights may be of interest in academic studies of nucleation and crystallization, since these cyclic polyglycolides (PGAs) mainly consist of extended-ring crystallites.

Author contributions

HRK – conceptualization, project administration, supervision, investigation, methodology, writing – original draft; SMW – investigation, methodology, data curation, visualization, writing – review & editing

Conflicts of interest

There are no conflicts to declare.

Data availability

Data for this article are available at Zenodo (**https://doi.org/10.5281/zenodo.16273078**).

Fig. S1 GPC elution curves of the PGAs No. 3A and 4A, Table 2. Fig. S2 GPC elution curve of PGA No. 7, Table 2. Fig. S3 MALDI TOF mass spectrum of PGA No. 9, Table 2. Fig. S4 MALDI TOF mass spectrum of PGA No. 11, Table 2. See DOI: https://doi.org/10.1039/d5py00762c.

Acknowledgements

The authors would like to thank Dr S. Rost (Elantas/Altana SE, Hamburg) for his financial support; S. Bleck (TMC, Hamburg) for performing the DSC measurements; and Dr A. Meyer (IPC, Hamburg) for performing the X-ray measurements. The authors also thank Dipl. Ing. A. Myxa (BAM, Berlin) for the GPC measurements.

References

1 J. A. Semlyen, *Cyclic Polymers*, Springer, 2000, pp. 1–46.
2 J. A. Semlyen, in *Large Ring Molecules*, ed. J. A. Semlyen, J. Wiley & Sons, Chichester, 1996, ch. 1.
3 N. Nasongkla, B. Chen, N. Macaraeg, M. E. Fox, J. M. Fréchet and F. C. Szoka, *J. Am. Chem. Soc.*, 2009, **131**, 3842–3843.
4 H. R. Kricheldorf, *J. Polym. Sci., Part A: Polym. Chem.*, 2010, **48**, 251–284.
5 J. N. Hoskins and S. M. Grayson, *Polym. Chem.*, 2011, **2**, 289–299.
6 N. Sugai, S. Asai, Y. Tezuka and T. Yamamoto, *Polym. Chem.*, 2015, **6**, 3591–3600.
7 N. Zaldua, R. Liénard, T. Josse, M. Zubitur, A. Mugica, A. Iturrospe, A. Arbe, J. De Winter, O. Coulembier and A. J. Müller, *Macromolecules*, 2018, **51**, 1718–1732.
8 R. Liénard, J. De Winter and O. Coulembier, *J. Polym. Sci.*, 2020, **58**, 1481–1502.
9 F. M. Haque and S. M. Grayson, *Nat. Chem.*, 2020, **12**, 433–444.
10 E. Louisy, G. Fontaine, V. Gaucher, F. Bonnet and G. Stoclet, *Polym. Bull.*, 2020, 1–21.
11 M. Kruteva, J. Allgaier and D. Richter, *Macromolecules*, 2023, **56**, 7203–7229.
12 H. R. Kricheldorf, S. M. Weidner and A. Meyer, *Mater. Adv.*, 2022, **3**, 1007–1016.
13 H. R. Kricheldorf, *Macromol. Rapid Commun.*, 2009, **30**, 1371–1381.
14 H. G. Buhrer and H. G. Elias, *Makromol. Chem.*, 1970, **140**, 41–54.
15 H. G. Elias and H. G. Buhrer, *Makromol. Chem.*, 1970, **140**, 21–39.
16 H. R. Kricheldorf, *Macromol. Chem. Phys.*, 1974, **175**, 3325–3342.
17 H. R. Kricheldorf and K. Bosinger, *Makromol. Chem.*, 1976, **177**, 1243–1258.
18 H. R. Kricheldorf, C. von Lossow and G. Schwarz, *Macromolecules*, 2005, **38**, 5513–5518.
19 H. R. Kricheldorf, C. Von Lossow and G. Schwarz, *Macromol. Chem. Phys.*, 2005, **206**, 282–290.
20 H. R. Kricheldorf, C. Von Lossow and G. Schwarz, *J. Polym. Sci., Part A: Polym. Chem.*, 2006, **44**, 4680–4695.
21 H. R. Kricheldorf, K. Bosinger and G. Schwarz, *Makromol. Chem.*, 1973, **173**, 43–65.
22 H. R. Kricheldorf and K. Bosinger, *Makromol. Chem.*, 1973, **173**, 67–80.
23 H. R. Kricheldorf, N. Lomadze and G. Schwarz, *Macromolecules*, 2007, **40**, 4859–4864.
24 H. R. Kricheldorf and J. M. Jonte, *Polym. Bull.*, 1983, **9**, 276–283.
25 H. R. Kricheldorf, N. Lomadze and G. Schwarz, *J. Polym. Sci., Part A: Polym. Chem.*, 2008, **46**, 6229–6237.
26 H. R. Kricheldorf, N. Lomadze and G. Schwarz, *J. Macromol. Sci., Part A:Pure Appl. Chem.*, 2009, **46**, 346–352.
27 A. K. Acharya, Y. A. Chang, G. O. Jones, J. E. Rice, J. L. Hedrick, H. W. Horn and R. M. Waymouth, *J. Phys. Chem. B*, 2014, **118**, 6553–6560.
28 H. A. Brown, Y. A. Chang and R. M. Waymouth, *J. Am. Chem. Soc.*, 2013, **135**, 18738–18741.
29 D. A. Culkin, W. H. Jeong, S. Csihony, E. D. Gomez, N. R. Balsara, J. L. Hedrick and R. M. Waymouth, *Angew. Chem., Int. Ed.*, 2007, **46**, 2627–2630.
30 W. Jeong, E. J. Shin, D. A. Culkin, J. L. Hedrick and R. M. Waymouth, *J. Am. Chem. Soc.*, 2009, **131**, 4884–4891.
31 G. O. Jones, Y. A. Chang, H. W. Horn, A. K. Acharya, J. E. Rice, J. L. Hedrick and R. M. Waymouth, *J. Phys. Chem. B*, 2015, **119**, 5728–5737.
32 E. J. Shin, W. Jeong, H. A. Brown, B. J. Koo, J. L. Hedrick and R. M. Waymouth, *Macromolecules*, 2011, **44**, 2773–2779.
33 X. Y. Zhang and R. M. Waymouth, *ACS Macro Lett.*, 2014, **3**, 1024–1028.
34 A. V. Prasad, L. P. Stubbs, M. Zhun and Y. H. Zhu, *J. Appl. Polym. Sci.*, 2012, **123**, 1568–1575.
35 Z. Luo, S. Chaemchuen, K. Zhou, A. A. Gonzalez and F. Verpoort, *Appl. Catal., A*, 2017, **546**, 15–21.
36 X.-Q. Li, B. Wang, H.-Y. Ji and Y.-S. Li, *Catal. Sci. Technol.*, 2016, **6**, 7763–7772.
37 G. F. Si, S. J. Zhang, W. M. Pang, F. Z. Wang and C. Tan, *Polymer*, 2018, **154**, 148–152.
38 R. W. Kerr, P. M. Ewing, S. K. Raman, A. D. Smith, C. K. Williams and P. L. Arnold, *ACS Catal.*, 2021, **11**, 1563–1569.
39 D. Gilding and A. Reed, *Polymer*, 1979, **20**, 1459–1464.
40 G. Benecke, W. Wagermaier, C. Li, M. Schwartzkopf, G. Flucke, R. Hoerth, I. Zizak, M. Burghammer, E. Metwalli and P. Müller-Buschbaum, *J. Appl. Crystallogr.*, 2014, **47**, 1797–1803.
41 S. M. Weidner, A. Meyer and H. R. Kricheldorf, *Eur. Polym. J.*, 2024, **207**, 112811.
42 H. Kricheldorf, S. Weidner and A. Meyer, *Polym. Adv. Technol.*, 2024, **35**, e6365.

43 H. R. Kricheldorf, S. M. Weidner and A. Meyer, *Polymer*, 2024, **309**, 127440.
44 H. R. Kricheldorf, S. M. Weidner and A. Meyer, *Macromol. Chem. Phys.*, 2024, **225**, 2300397.
45 Y. Bao, N. Paunović and J. C. Leroux, *Adv. Funct. Mater.*, 2022, **32**, 2109864.
46 P. J. Flory, *Chem. Rev.*, 1946, **39**, 137–197.
47 H. R. Kricheldorf and S. M. Weidner, *Polymer*, 2023, **276**, 125946.
48 S. M. Weidner, A. Meyer and H. R. Kricheldorf, *Polymer*, 2023, **285**, 126355.
49 Y. Chatani, K. Suehiro, Y. Ôkita, H. Tadokoro and K. Chujo, *Macromol. Chem. Phys.*, 1968, **113**, 215–229.